

SEASONAL VERTICAL WATER VAPOR DISTRIBUTION AT THE PHOENIX LANDING SITE

C. W.S. Leung, *Jet Propulsion Laboratory/Caltech, Pasadena, USA* (cecilia.leung@jpl.nasa.gov), **L. Tamppari**, *Jet Propulsion Laboratory/Caltech, Pasadena, USA*, **D. Kass**, *Jet Propulsion Laboratory/Caltech, Pasadena, USA*, **M. Smith**, *NASA Goddard Space Flight Center, Greenbelt, USA*, **G. Martínez**, *Lunar and Planetary Institute, Universities Space Research Association, Houston, USA*, **E. Fischer**, *University of Michigan, Ann Arbor, USA*.

Introduction:

The objective of this study is to use a combination of orbital and surface observations to constrain the seasonal vertical water vapor distribution at the Phoenix Mars Lander location (68°N, 234°E) in the Martian north polar region. The water cycle is key to understanding Mars' current and past climate, and the vertical distribution of water reflects the complex interactions involving temperature variations, winds, cloud microphysics, convective and turbulent mixing, regolith-atmosphere exchange, and other processes that influence the inventory of water. While remote sensing observations from orbit have provided a global, multi-year interannual climatology of water vapor column abundances in the Martian atmosphere [1,2,3,4], no such extensive climatology exists for the vertical distribution of water vapor. Furthermore, orbital assets typically have difficulties observing the bottom-most scale height due to limited path transmission resulting from increased dust and cloud optical thickness near the surface [5,6]. Thus, the vertical water vapor distribution particularly in the planetary boundary layer remains poorly constrained due to the limited direct observations.

A key emphasis of this study is the usage of a recently recalibrated surface vapor pressure dataset, provided by the of the Phoenix (PHX) thermal and electrical conductivity probe (TECP) [7]. These newly recalibrated measurements provide a new constraint for studying the vertical profiles of water vapor along with using coordinated measurements of water vapor column abundances from TES and CRISM, near-surface pressure and temperature from the Phoenix Meteorology Package (MET), and atmospheric profiles of temperature and water ice clouds from the Mars Climate Sounder (MCS). We will test whether modeled water vapor column abundances are consistent with the common hypothesis that water vapor distribution is well mixed from the surface to the cloud saturation level. Furthermore, this study will evaluate whether water may be enhanced or depleted in the near surface layer, and determine the maximum height of a well-mixed layer as a function of season for the duration of the Phoenix mission.

Observational Constraints:

For this study, we take a seasonal approach to understanding the vertical distribution of water vapor

between $L_s = 75^\circ$ to $L_s = 150^\circ$, partitioning this seasonal period into 5-degree solar longitude ($^\circ L_s$) bins.

Relative Humidity. The aggregate TECP dataset taken over the full duration of the Phoenix mission is shown in Figure 1. A diurnal cycle can be seen where peak water vapor pressure values occur during the mid-afternoon and drop to a minimum value ~ 0200 LTST. While relative humidity measurements were taken near continuously over the full diurnal cycle for a few individual sols, relative humidity measurements were typically observed for only a few hours each sol resulting in large gaps when looking at the full diurnal cycle for most individual sols. The mid-afternoon 1500 LTST TECP vapor pressure value extracted from each of the resulting diurnal curves is then used to represent the surface water vapor constraint in each seasonal bin.

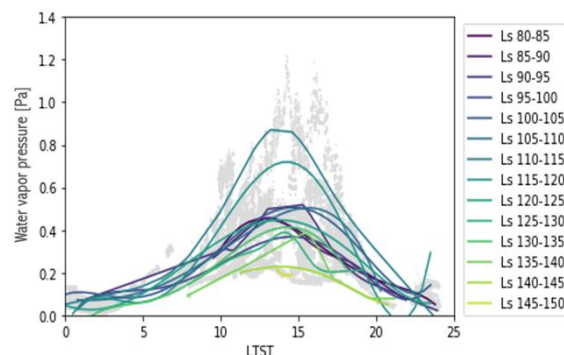


Figure 1. All TECP vapor pressure measurements collected over the 151 sols of the Phoenix mission are shown in grey. Overlaying the individual measurements are diurnal curves fitted to the TECP data in each $5^\circ L_s$ interval.

Water Vapor Column Abundance. We consider mid-afternoon measurements from TES and CRISM which fall within $\pm 5^\circ$ latitude and $\pm 15^\circ$ longitude of the Phoenix landing site. In our climatological approach, we consider the average water vapor column abundances taken across all Mars Years where measurements are available, even though interannual variability is present in the Martian water cycle. We partition the combined TES and CRISM data sets into $5^\circ L_s$ bins and find the average value of each bin as the representative water vapor column abundance at that

season. The seasonal trend in water vapor column abundances between $L_s \sim 30^\circ$ to 180° is shown in Figure 2. The overall historic seasonal trend indicates a gradual rise from ~ 22.8 pr- μm near the beginning of the Phoenix mission ($L_s \sim 76^\circ$), to a peak of ~ 37.8 pr- μm at $L_s = 125^\circ$, and then follows a relatively sharp drop in column water vapor until the end of the Phoenix mission.

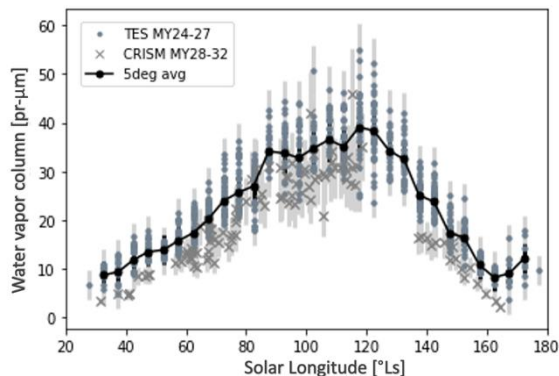


Figure 2. Seasonal column water vapor abundances for TES (MY 24-27) & CRISM (MY 28-32) over the Phoenix landing site. Black circles represent the 5° L_s binned average values. The seasonal trend of the binned average shows a gradual increase in water vapor starting in mid-northern spring, peaking at around $L_s=120^\circ$, then a sharper decrease towards northern autumn equinox.

Temperature Profile. The temperature profile is used to calculate saturation vapor pressures and determine saturation conditions at each atmospheric level. Above the boundary layer, the seasonal average temperature profile is determined from MCS temperature retrievals. For our seasonal study of water vapor variability at the Phoenix landing site, we generated a set of MCS profiles for each 5° L_s bin that included retrievals from both limb and nadir sounding based on a query matching local time between 1350 to 1650 LTST, 63° to 73°N latitude, and -135° to -115°E longitude. Between 216 to 301 individual MCS profiles were included for each seasonal bin, from which a mean MCS temperature profile was derived (Fig. 3). The average temperature profile in the lowest 1 to 1.5 scale height, depending on the season, is estimated using a combination of MCS surface temperatures, MET near-surface measurements, and from potential temperature profiles determined from column models and large eddy simulations at the Phoenix landing site. We incorporated a surface layer with the superadiabatic lapse rate, then a layer with an adiabatic lapse rate of 4.5 Kelvin per km, up to a height of 5.25 km, based on PHX EDL modeling work [8].

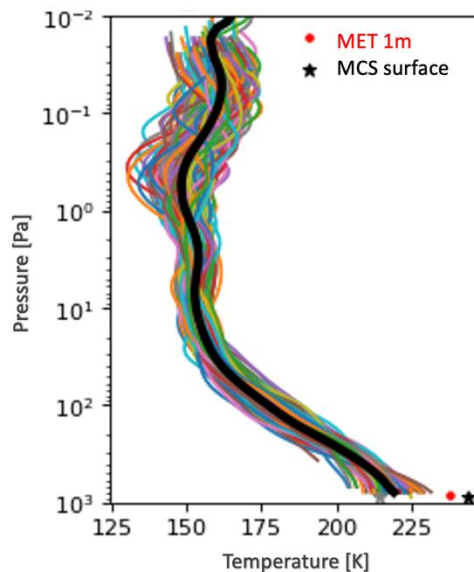


Figure 3. Temperature profile for the 5° L_s bin representing $L_s = 85-90^\circ$. The average MCS temperature profile (thick black line) was determined from 263 profiles between MY28 to 35 that satisfy our latitude-longitude-local time requirements.

Testing the Well-mixed Assumption for Vertical Water Vapor Distribution:

We test the validity of the uniformly well-mixed assumption of water vapor distribution by constraining the constant water vapor mixing ratio in the near-surface to that of the observed TECP water vapor pressure, then calculating the resulting total water vapor column abundance and comparing this value with the column vapor abundance as observed from orbit. A number of retrieval algorithms use the vertically uniform assumption to determine the column vapor abundances. We consider the water vapor profiles for two cases where water is well-mixed in the lowest atmospheric levels: one where the near-surface vapor mixing ratio is constant up to the saturation or cloud condensation level (CCL), and the other where the near-surface vapor mixing ratio is constant up to the top of the planetary boundary layer.

Well-mixed to the Cloud Condensation Level. To determine the water vapor profile for this first scenario, the observed TECP water vapor mixing ratio is assumed to be constant and well-mixed from the surface up to the cloud condensation level, and then follows the saturation vapor pressure curve to the top of the atmosphere. The saturation vapor pressure as a function of height is determined from the seasonally averaged temperature profile, as described above. The altitudes of the cloud condensation level varies with season, reflecting the observed vertical temperature seasonal variability. We found that the cloud

condensation height near the Phoenix landing site is ~ 15 km at $L_s \sim 90^\circ$ and decreases to ~ 8 km near $L_s = 125^\circ$.

Well-Mixed to the Top of the Boundary Layer. In the second scenario, vapor is well-mixed only to the top of the planetary boundary layer, falls off, and then follows a saturation vapor pressure curve. We assume the constant water vapor mixing ratio, constrained by the near-surface TECP value, extends from the ground up to the top of the boundary layer at 4 km altitude. Above the planetary boundary layer height, the water vapor vertical profile is represented by a diagonal transect, the slope of which is determined by the altitude it intersects with the inflection point on the saturation vapor pressure curve. Above this point, we assume the vapor follows the saturation vapor pressure curve to the top of the atmosphere.

Excess & Depleted Near Surface Layer. The total water vapor column abundance is determined by integrating the water vapor mixing ratio from the surface up to the top of the atmosphere. Figure 4 shows the resulting seasonal variability in modeled water vapor column abundances for case 1a (uniformly well-mixed to the cloud condensation level) and case 1b (uniformly well-mixed to top of the planetary boundary layer) compared to the water vapor column abundances observed from TES & CRISM with uncertainties.

The overall results show that, generally speaking, the assumption of a uniform water vapor mixing ratio from the surface up to the cloud condensation level and then following a saturation vapor pressure curve to the top of the atmosphere yields column abundances that are too high from the beginning of the Phoenix mission $L_s \sim 76^\circ$ to $L_s \sim 120^\circ$ and too low from $L_s \sim 120^\circ$ to the end of the Phoenix mission at $L_s \sim 150^\circ$, when compared to orbital measurements. A similar conclusion is found even when the uniformly well mixed water vapor extends only up to the top of the boundary layer (case 1b). This suggests that, prior to $L_s = 120^\circ$, there is an overabundance of water near the surface, concentrated at a height below that of the planetary boundary layer. After $L_s \sim 120^\circ$, this trend is reversed, suggesting that there is a layer above the surface layer that TECP measures that has a higher vapor mixing ratio, or stated another way, that the surface layer is depleted in vapor.

The timing of this transition is coincident with the peak water column abundances observed from orbit ($L_s = 110^\circ - 120^\circ$), when water ceases to increase in the polar atmosphere and begins to decrease again. Therefore, it may be that our determination of this seasonal overabundance of vapor followed by a depletion of vapor in the lower layer is caused by net outgassing of the surface from the beginning of the Phoenix mission through $L_s = 120^\circ$, which then transi-

tions to a net uptake of vapor into the surface until the end of the mission. The physical mechanism causing the net outgassing maybe due to either sublimation of shallow-subsurface ice escaping through the regolith to the atmosphere, and/or net desorption (regolith becoming drier over the pass of the sols). We also do not rule out the possibility of low-level advection of vapor-laden airmasses (presumably northerly) followed by advection of dry airmasses, or some combination of these mechanisms.

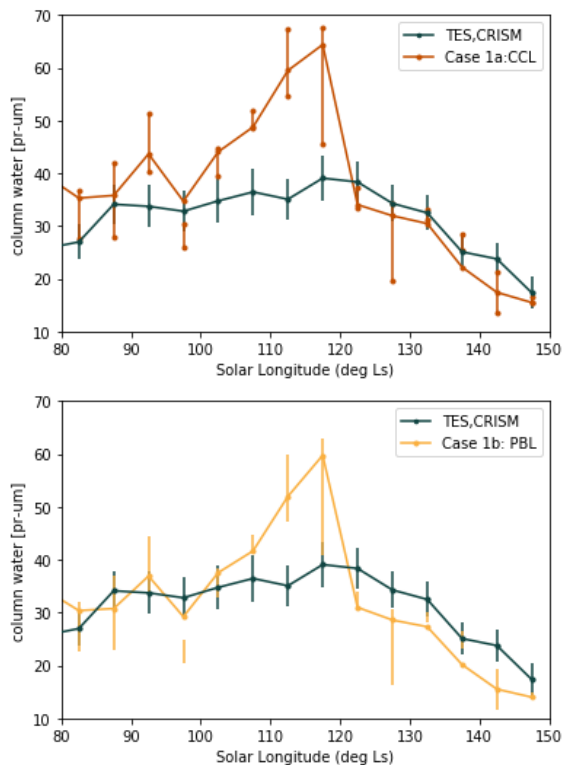


Figure 4. Seasonal variability in modeled water vapor column abundances for case 1a (uniformly well-mixed to the cloud condensation level), and case 1b (uniformly well-mixed to top of the planetary boundary layer) versus the vapor column abundances from TES & CRISM with uncertainties. The error bars on the TES-CRISM data represent ± 1 -sigma variability.

Maximum Well-Mixed Layer Height:

Using both the TECP water vapor pressure as a constraint at the surface, as well as TES and CRISM vapor abundances to constrain the total water vapor in the integrated column, we can determine the maximum height of the near surface well-mixed water vapor layer. We consider two scenarios to account for cases when the well-mixed assumption results in water vapor column abundances greater than those measured by TES & CRISM (which applies between $L_s = 75^\circ - 120^\circ$, and $L_s = 130^\circ - 135^\circ$), versus those cases where the uniformly well-mixed assumption results in water vapor column abundances less than those measured by TES & CRISM (which applies

between $L_s = 120^\circ$ - 130° , and $L_s = 135^\circ$ - 150°).

Our results show that the height of the maximum mixed layer tends to rise between $L_s = 75^\circ$ until it reaches the highest maximum height of 13.3 km at $L_s = 95^\circ$ - 100° (Fig. 5). The maximum mixed layer height then rapidly falls until it reaches the lowest value of 3.45 km around $L_s = 115^\circ$ - 120° . Between $L_s = 120^\circ$ to 150° , the maximum height of the near surface well-mixed water vapor layer stays fairly consistent with a value hovering around a mean value of 6.86 km.

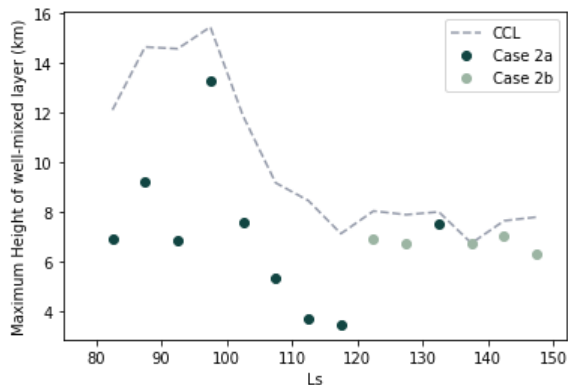


Figure 5. Seasonal variability in the maximum height of a well-mixed layer constrained by TES and CRISM total water vapor column abundances as well as by TECP representing the vapor quantity in the well-mixed region. The height of the cloud saturation level is plotted as the dash line in gray.

We compare our results with the values found in Pankine and Tamppari (2015), whose retrieval algorithm matched the combined daytime and nighttime TES water vapor spectral signatures for the same location and time period to determine the vertical extent of vapor in their ‘wet’ atmospheric layer and the value of the mixing ratio [9]. Their results found slight seasonal variability in the the height of the ‘wet’ layer in MY25, but remained mostly between 7–10 km from $L_s = 75^\circ$ and 140° , except during the period between $L_s = 90^\circ$ - 95° when it increased to 17 km (15-18km $L_s = 80^\circ$ - 100°). Considering the uncertainty of 2–3 km in Pankine and Tamppari (2015)’s retrieved ‘wet’ layer heights, our maximum well-mixed layer of 13.3 km at $L_s = 95^\circ$ falls only slightly below their lower limit, meanwhile, our maximum mixed-layer height of 7 km at $L_s = 140^\circ$ is well within their stated range. Interestingly, both our results and Pankine and Tamppari (2015) showed that the highest well-mixed layer heights during the period of the Phoenix mission could be expected around $L_s \sim 95^\circ$ - 100° .

Conclusion:

Using a combination of orbital and surface observa-

tions, we constrain the seasonal vertical distribution of water vapor in the planetary boundary layer and below the cloud condensation height the Phoenix Mars Lander location (68°N , 234°E) in the Martian north polar region. Previous observations have shown significant discrepancies regarding the vapor distribution in the boundary layer, drawing conflicting conclusions as to whether water is uniformly mixed below the cloud condensation height, or whether water is mostly confined in the near surface layer. We conclude that the uniformly well-mixed assumption leads to an over-estimation of the total water vapor column abundances from $L_s = 75^\circ$ - 120° , and an under-estimation of the total water vapor column abundances at $L_s = 120^\circ$ - 150° . The overestimation of vapor in the column is particularly evident during peak surface water vapor pressures ($\sim L_s = 110^\circ$ - 120°). We interpret this trend to mean there is a lower layer in which water is generally enhanced prior to $L_s = 120^\circ$ and depleted after $L_s = 120^\circ$. This suggests the possibility that this layer is owing to net vapor release from the surface prior to $L_s = 120^\circ$, such that daytime convective processes cannot mix it fast enough, and a concentration of water vapor at the surface that actively participates in subsurface exchange in a layer that is mostly decoupled from the daytime convective mixed layer. Further, it suggests the possibility that after $L_s = 120^\circ$, there is net adsorption of water into the surface, leaving behind a low-level deficit of water. Using both TECP and column vapor abundance as constraints for the vertical vapor distribution, we evaluated the maximum height of the well-mixed vapor layer to ranges between 3.45–13.3 km, with the lowest values during the time period of peak water vapor column abundances ($L_s = 110^\circ$ - 120°). Between $L_s = 120^\circ$ to 150° , the maximum height of the well-mixed layer remains fairly consistent with a mean altitude of 6.86 km. These results are particularly important for providing insight into the seasonal transport of water and the role of regolith-atmospheric exchange.

References:

- [1] Smith, (2002) *JGR: Planets*, 107(11), 1–19;
- [2] Smith, (2004) *Icarus*, 167(1), 148–165;
- [3] Smith et al., (2009) *JGR*, 114, 1–13;
- [4] Pankine et al., (2010) *Icarus*, 210, 58-71;
- [5] Kleinböhl et al., (2009) *JGR*, 114, E10006;
- [6] Guzewich et al., (2017) *JGR:Planets*, 122, 2779-2792;
- [7] Fischer et al., (2019) *JGR:Planets*, 124, 11, 2780-2792;
- [8] Tyler et al. (2008) *JGR*, 113, E00A12;
- [9] Pankine and Tamppari (2015) *Icarus*, 252, 107-120.